Effect of Molecule−Molecule Interaction on the Electronic Properties of Molecularly Modified Si/SiO_x Surfaces

Olga Gershewitz, Miri Grinstein, and Chaim N. Sukenik

Department of Chemistry, Bar-Ilan University, Ramat Gan, Israel 52900

Keren Regev, Jamal Ghabboun, and David Cahen*

Department of Materials & Interfaces, Weizmann Institute of Science, Rehovoth, Israel 76100

Received: June 21, 2003; In Final Form: October 23, 2003

We use the adsorption of systematically substituted silanes with either simple alkyl or alkyl phenyl ether chains onto oxidized Si to study the electronic effects of such molecular monolayers on Si. While there is no significant effect of distance of the substituents from the surface, a strong effect of what we interpret as depolarization is found for layers made up of molecules with high (>5 D) free molecule dipole moment. This is also apparent from differences in UV−visible and Fourier transform infrared (FTIR) spectral features, suggesting changes in molecular conformation, and, especially, from the measured contact potential differences. These reflect the modified surface's electron affinity and, thus, the effective dipole moment of the monolayer. The effect is ascribed to the system's response to the energetic price of dipole−dipole repulsion.

Introduction

Control over the surface chemistry and physics of a variety of solids can be achieved by the self-assembly of variously functionalized organic molecules onto their surfaces.[1,2] Silanes chemisorb onto an oxidized Si surface and form monolayers via self-assembly.[3,4] By systematically varying the functionality of these molecules, one can examine their effect on the surface's electronic properties [i.e., work function (WF), electron affinity (EA), band bending (BB), and surface recombination velocity[5]]. For oxidized Si this has been demonstrated in a preliminary study of Cohen et al.[6] on Si and in a number of studies on other semiconductors.[7]

In principle, the most straightforward effect is that of a molecular dipole on the semiconductor's electron affinity (or on the metal's work function). As long as we deal with a layer of dipoles with domains whose lateral dimensions (L) are much larger than the layer's width (d), the effect of the dipole layer on the measured surface potential can be gotten from the Helmholtz equation,[8,9] which gives the potential drop across the dipole film:

$$\Delta V = N\mu \cos\theta/\epsilon\epsilon_0 \qquad (1)$$

In this expression, N is the dipole density (per square centimeter), μ is the dipole moment (debyes),[10] θ is the *average* angle the dipole makes with the surface normal, ϵ is the effective dielectric constant of the molecular film (better viewed, for these monolayers, via the Clausius−Mosotti relation as an expression of the molecular polarizabilities), and ϵ_0 is the permittivity of vacuum.[9]

For the type of monolayers that are obtained by self-assembly of silanes on oxidized Si, $L \gg d$ will hold true.[11−13] In that case, one could argue that the actual distance of the dipole layer from the semiconductor surface is not important (cf. discussion in ref 14). While some of the earlier work that considered the effect of chain length of adsorbed saturated (alkyl) molecules on the resulting (Au) surface potential did find a clear dependence,[1,15] the results were less clear for arenethiols on Au.[16]

CHART 1. Molecules Used for Preparation of Monolayers on SiO_x

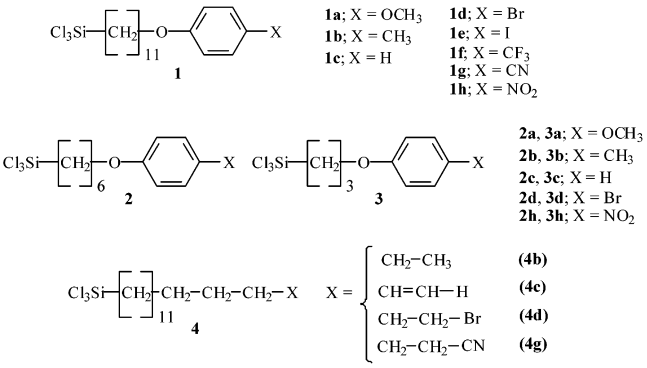

As part of an effort to optimize the design of maximally effective molecular absorbates, we focused the present study on a system that would allow convenient synthetic variation in creating appropriate building blocks for ordered siloxane-anchored monolayer films. Molecules of structure **1** mostly form well-packed siloxane-anchored monolayers, and the range of commercially available precursors provides for diverse functionality (see Chart 1). Homologues of **1**, in the form of molecules **2** and **3,** allow for systematic variation of the distance between the dipolar chromophore and the silicon surface. Molecules **4** provided for films of thickness comparable to those derived from molecules **1** with surfaces of comparable composition but lacking the aromatic ether moiety and its highly polarizable π-electron system.

Self-assembly of such molecules differs from the in situ displacement chemistry approach taken previously by us[6] and others,[17,18] where such chemistry provided access to a range of functionalized arrays. Both approaches have their advantages.

10.1021/jp035764q CCC: $27.50
Published on Web 12/13/2003

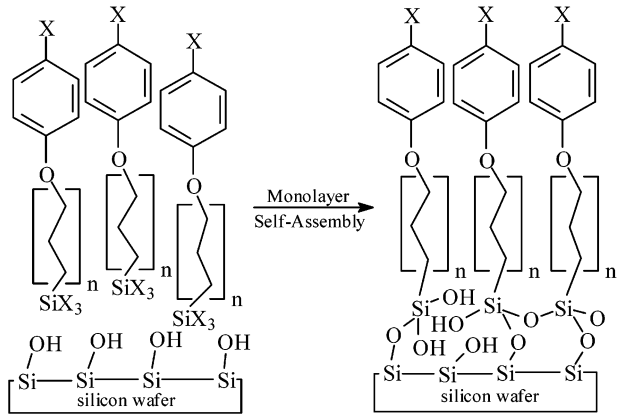

Figure 1. Schematic of self-assembly of functionalized siloxane-anchored films.

In the in situ transformation approach, all systems start with the same surface-bound entity, which provides the platform for the structural diversity. The main problem is that an in situ reaction may not go to completion and, thus, may produce a mixed monolayer. In the direct binding approach, variations due to differences in the efficiency of surface transformations (vide infra) are minimized, facilitating comparisons among differently substituted films. At first sight it would appear that the direct binding approach can suffer from possible differences in the way the modifying molecules attach to the surface, which could complicate things. However, for silanes this is unlikely, as it has been shown[13,19] that the alkyl chains in the silane monolayer are anchored to the SiO_x surface only occasionally; i.e., most of the chains are not bonded to the SiO_x (the chains are bonded between them via Si−O−Si bonds). This approach thus leads to a polymeric network of silane molecules, mostly bound to each other laterally rather than directly to the surface. This is important also for the relatively short molecules **2** and **3** that we use here, which are not expected to (and indeed do not) give very well-packed monolayers.

An idealized picture of the monolayer films that can result from the controlled self-assembly of silanes **1**−**3** is shown in Figure 1. Compounds **4** lead to films with simple polymethylene chains anchoring the functional group of interest.[20]

The composition, packing, and uniformity of the monolayer films were examined by advancing and receding contact angle measurements and by infrared (IR) and UV spectroscopies. The thickness of the films was measured by variable-wavelength ellipsometry and the observed thickness values were compared to the length of the fully extended molecular modifying agent. To examine the electronic properties of the modified Si surface, we measured the contact potential differences (CPD), in the dark and under saturating supra-band gap illumination, between the modified surface and a Au reference.[21−24]

While the band bending of the silicon substrate was strongly affected by the anchoring of the silanes to the oxidized surface, it did not show significant dependence on the molecular dipole of the adsorbates. We also did not find a significant effect on the surface potential if we varied the distance between the attached dipolar unit and the silicon surface. However, we did observe dependence, most clearly in terms of electron affinity of the surface, on the dipole moment of the modifying molecule. This trend breaks down for molecules with strongly electron-withdrawing substituents (especially CN and NO_2), something that we ascribe to depolarization, i.e., a saturation effect. This makes substituents far less effective in changing electron affinity than would be expected from the dipole moments of the free molecules. A preliminary account of this work has appeared.[25]

Experimental Section

Synthesis and Characterization of Molecules. The general synthetic scheme used to obtain silanes **1**−**3** is shown in Scheme 1.

Materials. Water was deionized and distilled in an all-glass apparatus. The following chemicals (≥99% pure unless indicated otherwise) were obtained from Aldrich: allyl bromide, trichlorosilane (distilled from quinoline immediately prior to use), *ω*-undecyl alcohol (98%), *p*-cresol, *p*-nitrophenol, *p*-bromophenol, *p*-iodophenol, α,α,α-trifluoro-*p*-cresol, phenol, *p*-methoxyphenol, Decalin, dicyclohexyl, hexane (AR), hexane (HPLC), acetone (AR), and hydrogen hexachloroplatinate (IV) hydrate. The 5-hexen-1-ol and methanesulfonyl chloride were obtained from Fluka. Compound **4b** (hexadecyltrichlorosilane) was purchased from Aldrich and was distilled before use. Compound **4c** was prepared according to ref 26, and compounds **4d** and **4g** were prepared as reported in ref 20.

Characterization of Synthesized Molecules. NMR spectra were obtained on samples dissolved in $CDCl_3$ by use of Bruker DPX 300 or AC 200 instruments. UV spectra were obtained, in solution, on samples dissolved in either ethanol or hexane (spectral grade) by use of quartz cuvettes in Cary Model 500 and Cary Model 100 spectrophotometers. Mass spectra were obtained by use of a Fisons VG Analytical AutoSpec E spectrometer in CI (methane) mode.

Synthetic Procedures (Scheme 1). The longer-chain mesylate ($n = 9$) was obtained as reported in ref 20. The shorter-chain version ($n = 4$) was prepared in an analogous fashion, with 5-hexen-1-ol substituted for *ω*-undecyl alcohol. The yield for this procedure was 73% (crude) and the material was used without further purification. The spectroscopic characterization of the ($n = 4$) mesylate is as follows: ^{1}H NMR δ (ppm): 5.82 (m, 1H), 5.0 (m, 2H), 4.23 (t, $J = 6.5$ Hz, 2H), 3.0 (s, 3H), 2.11, 1.76 (m, 2H), 1.52 (m, 2H). ^{13}C NMR δ (ppm): 137.72, 115.01, 69.86, 37.11, 32.81, 30.71, 24.44.

All of the phenoxy-containing olefins were prepared in identical fashion, from the appropriate phenol derivative and allyl bromide or one of the mesylates in a 1:1 molar ratio. The scale of these reactions was 30−50 mmol of starting materials. A typical procedure is as follows:

11-(4-Bromophenoxy)undec-1-ene. Into a dry 500-mL flask that was equipped with a magnetic stirring bar, a reflux condenser, and drying tube was placed 300 mL of acetone. To the flask was added *ω*-undecenyl mesylate (12 g, 48 mmol), potassium carbonate (6.69 g, 48 mmol), and *p*-bromophenol (8.3 g, 48 mmol). The reaction mixture was heated at reflux for 3 days and monitored by thin-layer chromatography (TLC) (hexane/ethyl acetate 90:10). It was cooled to room temperature and the resulting suspension was concentrated to a solid on a rotary evaporator. The material was suspended in ether and transferred to a separatory funnel, where it was washed with cold water, 5% NaOH, and saturated aqueous NaCl. It was then dried with $MgSO_4$, filtered, and concentrated on a rotary evaporator. The 11-(4-bromophenoxy)undec-1-ene (precursor of **1d**) was obtained as a yellow liquid and used after purification by chromatography (silica gel, hexane/ethyl acetate 90:10): yield 8.213 g (52.5%). ^{1}H NMR δ (ppm): 6.7 (m, 2H) and 7.3 (m, 2H), 5.8 (m, 1H), 5.0 (m, 2H), 3.94 (t, $J = 6.6$ Hz, 2H), 2.04 (m, 2H), 1.75 (m, 2H), 1.45 (m, 12H). ^{13}C NMR δ (ppm): 158.26, 139.21, 132.18 (2C), 116.30 (2C), 114.15, 112.55, 68.26, 33.82, 29.50, 29.42, 29.36, 29.18, 29.12, 28.94, 26.00. UV

SCHEME 1. Synthetic Pathway for Phenyl Ether Trichlorosilanes

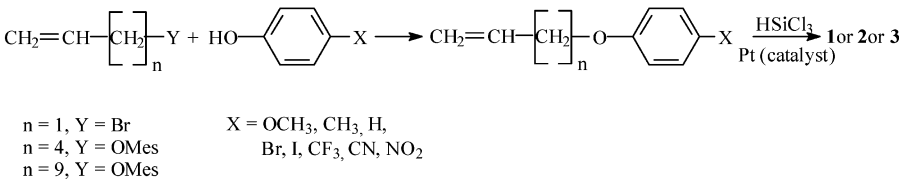

TABLE 1: Dipole Moments for the C11 Series of Molecules and Model Systems[a]

	dipole moment			
functional group	$(CH_3O)_3SiC_{11}-OC_6H_4X$[b]	$CH_3CH_2-OC_6H_4X$[b]	$CH_3CH_2-OC_6H_4X$[c]	$CH_3CH_2-OC_6H_4X$[d]
OMe syn/anti	−2.4/−0.2	−2.03/−0.18	−0.15[e]	
Me	−1.8	−1.12	−1.1	
H	−2.0	−1.21	−1.35	
Br	3.3	2.01	2.95	3.20
I	2.9	1.63	2.85[e,f]	3.10
CF_3	5.5	3.9	4.1	
CN	6.0	4.4	5.95	
NO_2	8.0	6.38	6.05	

[a] Calculated by use of various approximations. [b] PM3 semiempirical nonpolarization method.[27,29,30] [c] B3LYP-DFT cc-pVDZ full polarization method.[33,34] [d] B3LYP− DFT SDD (for I or Br) + cc-pVDZ (for all other elements) polarization method.[35] [e] See text. [f] Estimate.

(hexane): $\lambda_{max} = 228$, 283, 291 nm. UV (ethanol): $\lambda_{max} = 228$, 282, 290 nm. MS: 324.326 (found), 324.33(calcd).

The purification (distillation or chromatography), yields, and characterization of all of the remaining olefins are provided as Supporting Information.

The silanes (**1**−**3**) were prepared by hydrosilylating the corresponding olefin. A typical procedure is as follows:

11-(4-Bromophenoxy)trichlorosilylundecane (1d). Into a 20-mL pressure tube containing a magnetic stirring bar were placed 11-(4-bromophenoxy)undec-1-ene (1 g, 3.1 mmol), 3 mL of $HSiCl_3$, and 10−20 μL of a 4% solution of $H_2PtCl_6 \cdot 6H_2O$ in *i*-PrOH. All transfers were done under a nitrogen atmosphere. The progress of the reaction was followed by monitoring the disappearance of olefinic protons in the ^{1}H NMR spectrum. After the reaction was complete, the contents of the tube were transferred (under nitrogen) to a 25-mL round-bottom flask. Excess $HSiCl_3$ was distilled off and the product was isolated by kugelrohr distillation at 145 °C and 0.08 mm; yield 19%. ^{1}H NMR δ (ppm): 7.45 (m, 2H) 6.78 (m, 2H), 3.93 (t, $J = 7.9$ Hz, 2H), 1.68−1.85 (m, 2H), 1.50−1.65 (m, 2H), 1.18−1.5 (m, 16H).

The distillation conditions, yields, and characterization of the remaining silanes are provided as Supporting Information.

Surface Treatment and Molecular Assembly. Quartz microscope slides (QSI) and silicon wafers (n-type, phosphorus-doped, ⟨100⟩, 2−4 Ω·cm, Okmetic, Finland) were rinsed in chloroform, acetone, and ethanol for 30 s each and dried in a filtered nitrogen stream. Samples were then immersed into piranha solution [70:30 concentrated H_2SO_4/H_2O_2 (30% v/v)] at 80 °C for 20 min. Samples were then washed three times with deionized water and dried in a filtered nitrogen stream.

Freshly cleaned samples were immersed into a solution of compound **1** or **4** in dicyclohexyl (DCH) 1/200 (v/v) for 1 h under N_2. Samples were then taken out of the solution and cleaned by sonication in chloroform, often followed by additional rinsing in chloroform. All samples were then dried with a filtered nitrogen stream.

Freshly cleaned samples were immersed into a solution of compound **2** or **3** in Decalin 1/400 (v/v) for 2 h under N_2. Samples were then taken out of the solution, sonicated in chloroform for 3 min, and then rinsed in acetone, ethanol, and finally deionized (DI) water. For further cleaning, samples were washed with chloroform in a Soxhlet extractor for 2 h and then dried with a filtered nitrogen stream.

Tools for Monolayer Characterization: Contact angle measurements (advancing and receding) were done under ambient conditions with a Rame-Hart NRL goniometer. All samples were measured at least three times. Film thickness was measured on Si wafers with a Model M44 ellipsometer (J. A Woollam Co.). The measurements were done at 44 wavelengths between 680 and 1108 nm and were analyzed by the instrument's (VASE) software.

X-ray photoelectron spectroscopy was done on a Perkin-Elmer ESCA 5400 using an Al Kα source, at a base pressure of 10^{-9} Torr and a takeoff angle of 90°. High-resolution multiplex spectra were collected on a ∼2−3 mm spot, with 40 eV pass energy and a resolution of 50 eV. The spectrometer was calibrated according to standard procedures by use of Au $4f_{7/2}$ and Cr $2p_{3/2}$ peaks at 83.98 and 932.67 eV, respectively. The position of the peaks for the heteroatoms relevant to the monolayers were as follows: Br 3d, 70.8 eV; I 3d, 620.8 and 630.7 eV; F 1s, 688.4 eV; N 1s (nitro), 406.5 eV; N 1s (cyano), 399.4 eV.

Calculations of the molecules' lengths, to compare with film thickness deduced from ellipsometry, were done with PC-MODEL (Serena Software). These lengths were for the fully extended chain of the free molecules. The length used for comparison was from the silicon atom of the silane to the most remote atom on the other end of the chain. Dipole moments for various models of molecules, related to this study, were calculated by the PM3 semiempirical method (parametric method 3)[27,28] and the B3LYP (Becke 3-parameter hybrid exchange[29] with Lee−Yang−Parr correlation)[30] density functional theory (DFT) method using the Gaussian98 program package.[31] PM3 is a popular and quick method to calculate dipole moments for organic systems with an accuracy of ∼0.6 D.[32] This is sufficient if one is interested mainly in the *trend* of the dipole moments, as is the case for our system of molecules. We calculated the dipole moments for the molecules with a trimethoxysilane phenyl ether bound to different functional groups X (see above) and different chain lengths ($n = 3$, 6, 11). Table 1 shows results obtained with PM3 for $n = 11$, and for CH_3-terminated smaller molecules, for comparison with the DFT method. The dipole moment values and trend are only

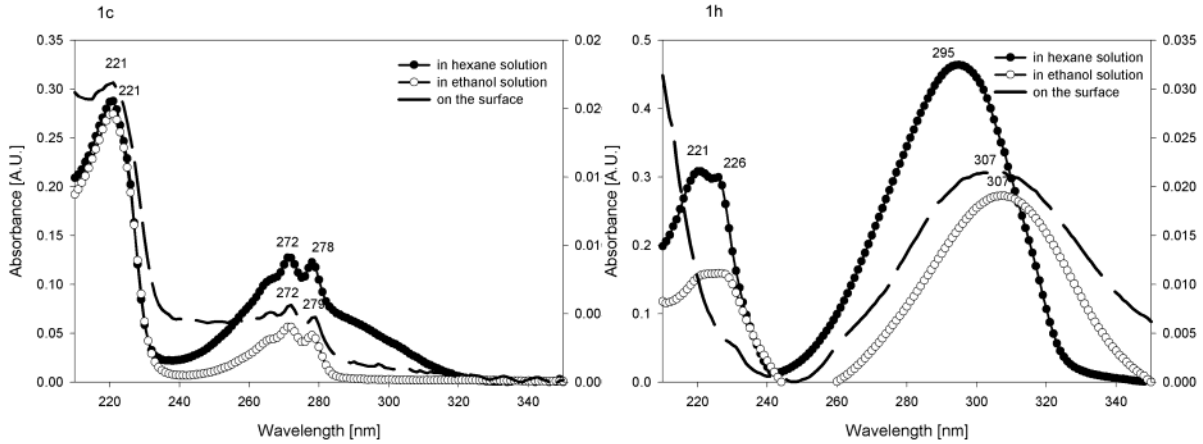

Figure 2. UV−vis spectra for olefin precursors to silanes **1h** and **1c** and films of these silanes, deposited on quartz substrates, measured in hexane, ethanol, and air (films).

weakly dependent on the number of carbons in the chain, which is why results for $n = 3$ and 6 are not shown separately.

To verify the trend found with the PM3 method, more accurate calculations were done on simpler model molecules with the B3LYP (DFT) method that incorporates electron correlation, with the contracted basis set cc-pVDZ (correlation-consistent polarized valence double-ζ).[33,34] To overcome the problem of this method with the iodine-substituted molecule (and its large number of electrons), we also made calculations using a combination of the SDD (Stuttgart/Dresden)[35] basis set with polarization functions on iodine and the cc-pVDZ basis set for the other elements. This was done for both the Br- and the I-substituted molecules, to get an idea of the differences between them. This difference was then used to *estimate* the dipole moment of the I-substituted molecule (with all cc-pVDZ). For the methoxy-substituted compounds, two conformations (syn and anti) of nearly equal energy are possible. Dipole calculations for both conformers are given, except in the case of the full polarization method, where the results were not significantly different between the two.

Infrared (ATR-FTIR) spectra were obtained on a Bruker Vector 22 spectrometer. Spectra of the as-deposited films were collected with a 60 × 20 × 0.45 mm Si parallelogram prism, prepared in-house by polishing the two short edges of a freshly cut double-side polished silicon wafer to a 45° angle. The background was collected after the piranha treatment of the cleaned ATR prism, and the sample collection was done after monolayer film deposition. A background spectrum of the clean ATR prism was subtracted from each sample spectrum. Typically, we collected 44 scans at 4-cm^{-1} nominal spectral resolution.

UV−vis spectroscopy was used to examine the olefin precursors of silanes **1**−**3** (no data were obtained for compounds **4**, which lack the aromatic ring) in solution. The surface films obtained from the self-assembly of **1**−**3** as films deposited on quartz were examined by UV−vis spectroscopy on a Cary Model 100 or Model 500 spectrometer (in double-beam transmission mode). Spectra were run against a reference sample of untreated quartz (that had also been cleaned in piranha solution). All samples were measured in the wavelength range of 200−500 nm.

Kelvin probe measurements were performed to determine the work functions of the modified surfaces. The work function is calculated from the contact potential difference (CPD) between that of an unknown sample and a Au vibrating grid.[23,24]

TABLE 2: Features of UV Spectra, Measured in Ethanol and Hexane, for Olefin Precursors to Silanes 1−3, and Films of These Silanes, Deposited on Quartz Substrates

material	in solution of hexane (nm)	in solution of ethanol (nm)	as film on quartz (nm)
1a, **2a**, **3a** (CH_3O)	226, 290, 300	226, 290, 300	234, 295, 302
1b, **2b**, **3b** (CH_3)	224, 279, 286	225, 279, 286	228, 281, 287
1c, **2c**, **3c** (H)	221, 272, 278	221, 272, 278	221, 272, 279
1d, **2d**, **3d** (Br)	228, 283, 291	228, 282, 290	232, 285, 292
1e (I)	235, 281	235, 281	235, 282
1f (CF_3)	226, 269, 276	227, 270, 277	227, 270, 281
1g (CN)	245, 274, 283	250, 276, 286	250, 276, 286
1h (NO_2)	221, 226, 295	222, 226, 307	307

The CPD measurements were done with a Besocke Delta Phi commercial setup.[22] The sample and the probe were placed in a closed metallic box used as a Faraday cage in order to avoid electrical interference from external sources. The measurements were done in the dark and under photosaturation conditions [with a 360 W quartz tungsten halogen (QTH) lamp, intensity at the samples 130 mW/cm^2]. Surface band bending was calculated by subtracting the CPD values measured in the dark from those measured under photosaturation conditions.[24] The measurements of surface films obtained from the self-assembly of **1** and **4** were done open to air (humidity 45%, $T = 23$ °C). The measurements of surface films obtained from the self-assembly of **2** and **3** were in a glovebox dried with dry N_2 gas flow for at least 1 h before use. All samples were measured after measurement of a gold sample used for calibration and reference.

Results

The molecular environment created by the deposition of compounds **1**−**3** was probed by UV−vis spectroscopy (Table 2, Figure 2). The packing and order of the films was assessed by a combination of FTIR (position of CH_2 peaks and tilt angle), wetting measurements (advancing and receding water contact angles and hysteresis), and ellipsometry (thickness vs calculated length of extended chain and tilt angle). The characterization of films made from compounds **4** (except **4b**, which is very similar to the well-studied OTS (octadecyltrichlorosilane) monolayer[36]) has been reported elsewhere: **4d,g** in ref 20, **4c** in refs 37 and 38, and homologues of **4c** in ref 39.

Table 2 summarizes the UV data obtained from both the phenyl ether-bearing films and from solutions of their olefin precursors (as reference spectra for the expected peak positions in the anchored films). The UV spectra in solution demonstrate

TABLE 3: Summary of FTIR Spectra and Tilt Angles, Deduced from Variable Angle Ellipsometry, for Molecules of Groups 1 and 4

	FTIR for group **1**			FTIR for group **4**		
precursors	CH_2 antisym stretch, cm^{-1}	CH_2 sym stretch, cm^{-1}	tilt angle Θ,[a] deg	CH_2antisym stretch, cm^{-1}	CH_2 sym stretch, cm^{-1}	tilt angle Θ,[a] deg
a (OCH_3)	2921	2851	26			
b (CH_3)	2921	2851	25	2919	2850	21
c (H)	2921	2851	24	2921	2851	20
d (Br)	2921	2852	26	2920	2851	23
e (I)	2921	2852	26			
f (CF_3)	2923	2852	28			
g (CN)	2924	2852	29	2923	2852	25
h (NO_2)	2924	2853	30			

[a] Tilt angle, calculated from dichroic ratio by spectra of polarized IR.[40,41]

TABLE 4: Summary of Film Thicknesses, Deduced from Ellipsometry and Theory, for Molecules of Groups 1 and 4

	compounds **1**			compounds **4**		
terminal substituent	ellipsometric thickness (nm)	PC model chain length (nm)	calculated thickness[a]	ellipsometric thickness (nm)	PC model chain length (nm)	calculated thickness[a]
a (OCH_3)	1.94	2.28	2.05			
b (CH_3)	1.97	2.16	1.96	2.01	2.16	2.02
c (H)	1.94	2.06	1.88	1.97	2.12	1.99
d (Br)	2.09	2.13	1.91	2.05	2.13	1.96
e (I)	2.13	2.13	1.92			
f (CF_3)	2.23	2.29	1.98			
g (CN)	2.12	2.19	1.93	2.09	1.90	1.72
h (NO_2)	2.37	2.14	1.87			

[α] Thickness was calculated from θ (tilt angle) and the theoretically calculated molecular length. The tilt angle was calculated from the dichroic ratio by use of experimental polarized ATR-FTIR spectra.

TABLE 5: Summary of Contact Angle Measurements[a] on Films, Prepared from Silanes Series 1−4

precursors	**1** (C_{11}) contact angle adv/rec/hyst	**2** (C_6) contact angle adv/rec/hyst	**3** (C_3) contact angle adv/rec/hyst	**4** contact angle adv/rec/hyst
a (OCH_3)	76/73/3	83/78/5	82/77/5	
b (CH_3)	95/93/2	94/86/8	97/87/10	117/113/4
c (H)	90/86/4	89/82/7	91/82/9	103/100/3
d (Br)	89/84/5	93/86/7	93/85/8	92/88/4
e (I)	91/85/6			
f (CF_3)	101/94/7			
g (CN)	81/68/13			70/63/7
h (NO_2)	83/73/10	86/80/6	84/74/10	

[a] All values are given in degrees; adv = advancing, rec = receding, hyst = hysteresis.

the characteristic absorptions for the functional groups involved and show little or no variation with changes in the solution environment from hexane to ethanol [except for the cyano-substituted phenyl ether, which shifted from 245/274/283 nm (hexane) to 250/276/286 nm (ethanol), and the nitro-substituted phenyl ether, whose long-wavelength absorption shifted from 293 nm (hexane) to 308 nm (ethanol)]. The spectra of the self-assembled films were recorded with quartz substrates. All of these materials showed a short-wavelength absorption between 221 and 236 nm and a set of peaks at longer wavelength between 270 and 309 nm. In the surface films, the positions of these bands are virtually the same as those found in ethanol solution, with the exception of the methoxy-substituted system. Both the similarity to ethanol and the uniqueness of the methoxy system will be discussed below.

From the FTIR spectra we can estimate the degree of order in the monolayers from the asymmetric and symmetric stretches of the methylene groups. In Table 3 we present the symmetric and antisymmetric stretching frequencies for molecules **1**. In Table 4 we give the films' thickness values, as derived from ellipsometric data. These are compared to the expected film thickness, based on the calculated extended-chain molecular conformation and the tilt angle data from the FTIR. For the longer chains (**1** and **4**), the ellipsometry tracked well with the calculated chain lengths, except for the NO_2 derivative. With films derived from the shorter chain length materials **2** and **3,** the thickness values were more scattered. The significance of these results will be discussed later.

Results of the contact angle measurements on films prepared with silanes **1**−**4** are given in Table 5. The CH_3 and especially the CF_3 derivatives show higher contact angles than the other derivatives, which indicates that indeed these (hydrophobic) functional groups are facing outward in the monolayers. Likewise, the more hydrophilic CN and OMe derivatives show smaller contact angles. For the OMe, Me, H, and Br derivatives the wetting data show slightly larger hysteresis for the films derived from the shorter-chain compounds than in those obtained with the longer-chain molecules. For the CN and NO_2 derivatives, however, also the layers made from **1** show high hysteresis. Replacing the phenyl ring (in **1**) by CH_2 groups (in **4**) accentuates both the hydrophobicity (of the CH_3 and H derivatives) and the hydrophilicity (of the CN derivative) of the layers.

Evaluation of the electronic interaction between the ligands and Si surface was done by measuring their effect on the surface potential. The dipole-induced changes in EA were deduced from contact potential differences. Those give the difference in work

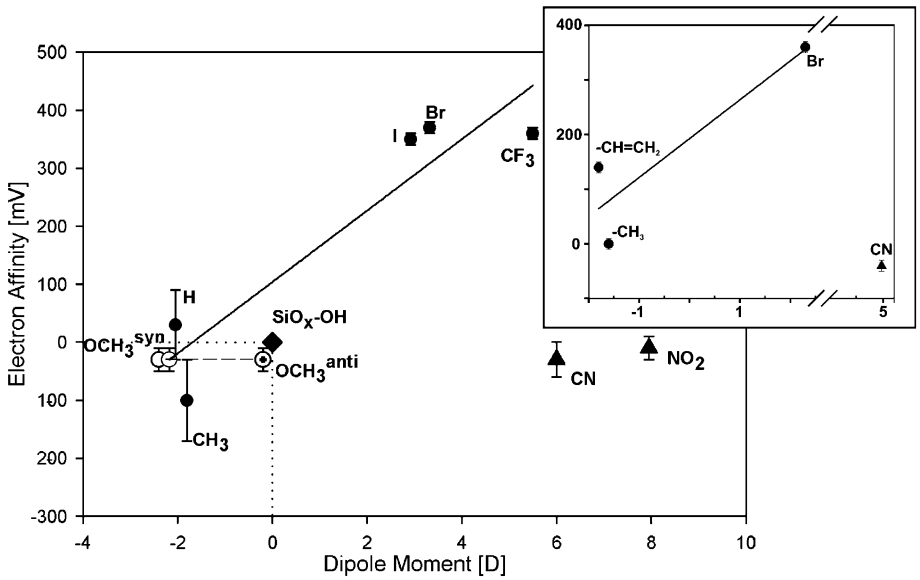

Figure 3. Measured contact potential differences (plotted as electron affinity) vs the dipole moments of the free molecules, calculated by the PM3 method. The main window shows the plot for surfaces modified with monolayers of compounds **1a**−**1h**, and the inset shows those for surfaces modified with monolayers of compounds **4b**−**4g.** The electron affinities that are plotted are WF_L (**4b**) − WF_L (sample). The best-fit line (R^2 = 0.891) shown includes all substituents except for CN and NO_2 and uses a dipole moment for CH_3O calculated for a 90:10 mixture of the syn and anti conformations (the open circle that falls on the solid line in the main figure).

function between the sample and a reference (Au, in our case). By doing the measurements under near-flat band conditions, i.e., under saturating supra-band gap illumination, where band-bending effects are minimized, the results allow a reasonable approximation to the electron affinity (except for the constant difference in energy between the Fermi level and the conduction band in the bulk, which is some 0.25 eV for the Si used here[42]). To ascertain that flat band conditions are approached, measurements are made on the sample as it is illuminated with increasing light intensities, until indication for saturation of the CPD is observed.[24,43]

In Figure 3 we plot data from Table 6 as the electron affinity for the Si/SiO_x surfaces, modified by adsorbing monolayers of **1,** relative to the electron affinity of the surface modified with monolayers of the unsubstituted alkylsilane **4b**, as a function of the calculated dipole moments of the geometry-optimized free molecules (cf. also Table 1). The irregular behavior of the NO_2 and CN substituents (**1g**,**h**) compared to that of all the others is immediately evident. The line shown is for the best linear fit (R^2 = 0.891) of a data set that ignores CN and NO_2 and treats CH_3O by using the mix of conformers (90% syn, 10% anti) that gives the best fit to the rest of the data.

As can be seen in Table 6, no strong difference exists between the band-bending values for the different surfaces, except for the strong reduction upon silanization, as compared to the bare SiO_x surface (which is most likely hydroxylated). This is similar to what we observed earlier,[6] although here the effect is even stronger (>400 mV vs 200−300 mV). The CF_3-, CN-, and NO_2-substituted molecules all seem to give slightly stronger band-bending than the other molecules.

TABLE 6: Results of Kelvin Probe Measurements, on *n*-Si Samples with Self-Assembled Monolayers of Silanes 1−4[a]

KP results for sample	WF_D[b] (eV)	WF_L[b] at photosaturation (eV)	BB[b] (V)	dipole moment calculated by PM3[c] (D)
Si-OH	−4.86 ± 0.06	−4.34 ± 0.05	0.52 ± 0.06	
SAM (**1a**)	−4.78 ± 0.04	−4.72 ± 0.02	0.066 ± 0.02	−2.4/−0.2
SAM (**1b**)	−4.71 ± 0.09	−4.65 ± 0.07	0.057 ± 0.02	−1.8
SAM (**1c**)	−4.84 ± 0.05	−4.78 ± 0.06	0.059 ± 0.01	−2.1
SAM (**1d**)	−5.20 ± 0.01	−5.12 ± 0.01	0.072 ± 0.01	3.3
SAM (**1e**)	−5.15 ± 0.01	−5.10 ± 0.01	0.050 ± 0.005	2.9
SAM (**1f**)	−5.19 ± 0.01	−5.11 ± 0.01	0.082 ± 0.005	5.5
SAM (**1g**)	−4.79 ± 0.04	−4.72 ± 0.03	0.069 ± 0.01	6.0
SAM (**1h**)	−4.84 ± 0.01	−4.74 ± 0.02	0.103 ± 0.10	8.0
SAM (**2a**)	−4.50 ± 0.03	−4.40 ± 0.01	0.10 ± 0.03	−3.6
SAM (**2b**)	−4.50 ± 0.03	−4.40 ± 0.01	0.10 ± 0.03	−2.6
SAM (**2c**)	−4.65 ± 0.04	−4.50 ± 0.04	0.15 ± 0.02	−2.8
SAM (**2d**)	−5.05 ± 0.09	−4.95 ± 0.09	0.10 ± 0.03	3.6
SAM (**2h**)	−4.75 ± 0.03	−4.60 ± 0.03	0.15 ± 0.03	7.8
SAM (**3a**)	−4.60 ± 0.03	−4.45 ± 0.01	0.15 ± 0.03	−2.0
SAM (**3b**)	−4.45 ± 0.03	−4.35 ± 0.01	0.10 ± 0.02	−1.9
SAM (**3c**)	−4.70 ± 0.04	−4.55 ± 0.03	0.15 ± 0.02	−2.2
SAM (**3d**)	−4.95 ± 0.09	−4.90 ± 0.09	0.05 ± 0.03	3.5
SAM (**3h**)	−4.60 ± 0.03	−4.50 ± 0.03	0.10 ± 0.03	8.2
SAM (**4b**)	−4.81 ± 0.01	−4.75 ± 0.01	0.057 ± 0.01	−1.6
SAM (**4c**)	−4.96 ± 0.01	−4.89 ± 0.01	0.073 ± 0.01	−1.8
SAM (**4d**)	−5.20 ± 0.01	−5.11 ± 0.01	0.086 ± 0.01	2.3
SAM (**4g**)	−4.74 ± 0.01	−4.71 ± 0.01	0.032 ± 0.01	5.0

[a] Measurements were taken of their contact potential differences vs Au (for which 5 eV was assumed as work function), in the dark and under saturating supra-band gap illumination. The dipole moments are those, calculated for the free molecules. [b] Errors are averages, derived from the actual experiments. The relatively small BB errors compared to the errors in the CPD and CPD_L values are due to the fact that these are averages derived from individual experiments (i.e., reflect the uncertainty in the determination of the change in CPD upon photosaturation). [c] The values for the dipole moments given here are for the molecules in Table 1 and the related text. The underlined values will be a particular focus of the discussion.

Discussion

We set out to investigate molecular dipole effects on the surface potential of (oxidized) Si substrates, by looking at the properties of the adsorbed monolayers and of the resulting modified surfaces. For the monolayers, we looked at their optical and vibrational properties and at their wetting behavior, while for the modified silicon, we concentrated on the surface potential. By adsorbing molecular monolayers on a semiconductor rather than on a metallic surface, we can gain information not only about the dipole of the monolayer but also about any net charge redistribution upon adsorption at the molecule/substrate interface (via the band-bending measurements),

something that is not possible with metal substrates. This is because band bending in the semiconductor is directly related to the charge on its surface. Whenever that net charge changes, the charge that neutralizes it, within the space charge, will change with it and so will the electrical potential gradient that results from this separation of charges and, thus, the band bending.

Phenyl ether-based chromophores were selected because of the relatively simple synthesis of a series of compounds, systematically varying both chain length and terminal substituent, so as to be able to draw conclusions concerning actual molecular effects. Within experimental error, we do not see significant differences (other than film thickness) among the phenyl ether monolayers as a function of the different polymethylene chain lengths. For a given terminal substituent, contact angles for wetting showed some differences related to the uniformity of the surface layer, while electronic and vibrational spectra and their surface potential (electron affinity and band bending) were nearly identical.

ATR-FTIR, ellipsometry, and UV−vis spectroscopic measurements showed that the extent to which the molecules formed well-packed monolayers on the surface varied as a function of their terminal substitution. From the data in Tables 3−5 we conclude that the molecules form a surface film that is roughly one monolayer thick with comparable coverage for all molecules from series **1**−**4**. XPS confirmed that the Br, I, CF_3, CN, and NO_2 compounds have their headgroups exposed. However, in the case of the CN and NO_2 derivatives, we see evidence for structural differences in the monolayers. The hysteresis between receding and advancing contact angles more than doubles and the advancing contact angles are particularly low. We interpret the lower advancing angle as being due to the presence of particularly hydrophilic functional groups. The high hysteresis implies inhomogeneous coating of the SiO_x surface.

In the CN and NO_2 derivatives, there are also small (2−3 cm^{-1}), but significant, shifts in the symmetric and asymmetric CH_2 IR stretching frequencies. On the basis of previous studies, which have shown that the position of the $\nu_a(CH_2)$ band is sensitive to the degree of conformational order (or crystallinity) of organic thin films,[44] we interpret these as an indication of a decrease in the order of the films. Also, the tilt angle of the molecules in the monolayer, deduced from the polarized ATR-FTIR data, decreases for the systems with these high dipole moment molecules (from 65 ± 1° for **1a**−**e** to 61 ± 1° for **1g** and **1h**). This can explain why the measured thickness of the monolayers of these molecules is less than that calculated for monolayers made up of molecules with fully extended chains. All this points to less average order for the NO_2 and CN monolayers than for the others.

Comparing the UV−vis measurements in apolar solvent (hexane) with those in polar (ethanol) solvent (Figure 2 and Table 2), we see that in the more polar medium (ethanol) the spectra of the very polar molecules (with -CN and -NO_2 substituents) are shifted to longer wavelength (lower energy). This shift can be understood by noting that the excited electronic states of these molecules are typically more polar than their ground states and thus the energy of the electronic excitation is less in a polar medium since that medium better stabilizes the excited state than the ground state.[45,46] The monolayer spectrum can then be explained by assuming that the immediate environment in the monolayer has some polar character, i.e., resembles the molecule's environment in ethanol more than that in hexane.

Comparing the spectrum of the film made with the methoxy-substituted molecule with its solution spectrum reveals an interesting feature. Based only on considerations of polarity, the shift between film on one hand and solvent spectrum on the other hand is consistent with a shift in the syn/anti conformer ratio, toward a preference for the syn conformer within the monolayer array. If the nearly equienergetic mixture of conformers in solution (approximately 50:50) shifts toward the more polar syn conformer in the monolayer, this would create a relatively polar local environment, consistent with the shift of the UV absorption to longer wavelengths. The spectral shift to longer wavelengths may also reflect an inherent difference between the spectra of the syn and anti conformers. Such favoring of the syn conformer is also suggested by the CPD results. Calculations to establish the preferred conformation of the methoxy group within an ordered surface might shed light on this issue; however, they were beyond the scope of this work.

Table 6 gives the changes in ϕ_{Au} and ϕ_{SC} in the dark and under illumination for the four series of molecules. The CPD data are with respect to the work function of the Au reference probe, ϕ_{Au}, which is taken as +5.00 eV, i.e., 5 eV below the vacuum level. With ϕ_{SC} as the work function of the semiconductor, CPD_d the value obtained in the dark, CPD_L the value obtained under illumination, and χ_{SC} the electron affinity of the modified Si,

$$CPD_d = \phi_{Au} - \phi_{SC} \tag{2a}$$

$$CPD_L = \phi_{Au} - \chi_{SC} \tag{2b}$$

so that

$$\chi_{SC} = CPD_L - \phi_{Au} \tag{3}$$

and

$$BB = CPD_L - CPD_d \tag{4}$$

We expect that adding a monolayer of molecules with a positive dipole (for electron-withdrawing substituents, Br, Cl, I, CF_3, NO_2, and CN) will increase the effective electron affinity of the free surface, whereas use of a negative molecular dipole for electron-donating substituents (OMe and Me) will decrease it. (The sign of the molecular dipole is taken to be negative if the positive pole of the dipole points away from the binding group). The change in surface potential (ΔV, in electronvolts) due to the dipole (μ) density, N, on the surface can be expressed by eq 1. In Figure 3 we plot the relative electron affinity (EA) of the oxidized Si, modified by the molecules from series **1**, as a function on the dipole moment of the substituent on the phenyl ether group (calculated by the PM3 method). We use the electron affinity, relative to that of **4b**, to try to isolate the effect of the molecular substituents on the phenyl ether (i.e., to exclude the effect of the silane modification of the SiO_x surface). This plot (and the similar ones that are obtained for series **2** and **3)** as well as that of series **4** (see inset in Figure 3) clearly show that something strange occurs with the NO_2- and CN-modified monolayers. Looking at Table 1, we see that the free molecules with these substituents have very high dipole moments. Upon packing of such molecules into a monolayer array, the increasing dipole−dipole repulsion will lead to decreased coverage and/or other changes to minimize this repulsion. A simple, Le Chatelier principle-compatible way to do this is to have the film modify itself so as to reduce the dipole moment/molecule. Indeed, something akin to this is what happens with inorganic systems, the best known of which is Cs on GaAs or Si.[47−50] At low coverage Cs (Cs−O, actually) donates an electron to the semiconductor and a strong dipole is formed, which is measured

TABLE 7: Calculated Values of Dipole Moment vs Experimental Results of the Change of Surface Potential, and Calculated Values of the Change of Surface Potential vs Theoretical Dipole Moment of Different Molecular Substituents

X[a]	ΔV_{exp}[b] (volts)	$\mu_{predicted}$[c] (D)	μ_{theory}[d] (D)	$\Delta V_{predicted}$[e] (V)	$\Delta\mu$[f] (D)	$\Delta(\Delta V)$[g] (volts)
OMe	−0.03	−0.15	−2.4/−0.2	−0.5/−0.04	−2.25/−0.05	−0.47/−0.01
Me	−0.10	−0.45	−1.8	−0.4	−1.35	−0.3
H	0.03	0.15	−2.0	−0.45	−2.15	−0.48
Br	0.37	1.75	3.3	0.70	1.55	0.33
I	0.35	1.65	2.9	0.6	1.25	0.25
CF_3	0.36	1.7	5.5	1.15	3.8	0.79
CN	−0.03	−0.1	6.1	1.3	6.2	1.33
NO_2	−0.01	−0.05	8.0	1.65	8.05	1.66

[a] Molecular substituents. [b] From CPD_l (with monolayer) − CPD_l (**4b**); sample **4b** is used as reference. [c] Dipole moment (in debyes; 1 D = 3.34 × 10^{-30} C·m), calculated from eq 1, with ΔV_{exp}. [d] Dipole moments, calculated by the semiempirical PM3 method, after geometry optimization, in the energy-minimized, fully extended position of the chain. [e] Calculated from μ_{theory} in eq 1. [f] $\Delta\mu$ = theory − predicted. [g] $\Delta(\Delta V)$ = predicted − experimental.

as a strong change in surface potential (so strong that in the case of GaAs a so-called negative electron affinity surface results). As Cs coverage increases, the change in surface potential becomes less until this change actually becomes negative, i.e., part of the original change is negated. This is explained by a return of some of the donated charge from the semiconductor surface to the Cs, so as to decrease the very strong dipole that was formed. In our case other avenues for decreasing the dipole are open to the system, because of the larger number of degrees of freedom of the molecular monolayer as compared to the atomic Cs one. Our data show that the molecules actually deform. While the data are not sufficiently clear to say how, it is likely that the deformations result in decreased dipole moment conformations, e.g., by bending of the molecules. It is remarkable that for the C3 and C6 series (**2** and **3)** similar effects are seen as for the C11 series. However, consistent with the expectation that the packing order in monolayers made up of the C6 and especially the C3 molecules is less than for the C11 films,[51−54] the slope of such an effect (as plotted from data in Table 6) changes according to C11 > C6 > C3. That is, the smaller changes in CPD_L between the bare surface and monolayers made with **2** (C3) molecules and, less so, with **3** (C6) molecules are consistent with less order with decreasing chain length.

Analyzing the data for the methoxy-substituted molecules is made more complex by the existence of two conformations with dipoles that differ by ∼2 D. The CPD data for the OCH_3 material (**1a**) are given twice in the plot, once with the dipole calculated for the syn conformer and once for the anti. The best-fit line for these data (not including the -CN and -NO_2 data points) was initially calculated ($R^2 = 0.87$) ignoring the CH_3O data. This line crossed a horizontal connecting the data points for the two CH_3O conformers at an isomer composition of 90% syn and 10% anti. When a dipole value with this weighted average was used, the best-fit line (shown) has a fit of $R^2 = 0.891$. This fit would be indistinguishable from mixtures with as little as 85% or as much as 96% syn. If the CF_3 data are grouped with the CN and NO_2 and eliminated from the correlation, the mix of CH_3O conformers optimizes at 80% syn ($R^2 = 0.94$). Either way, the suggestion of a monolayer surface enriched in molecules with a syn conformation is consistent with the discussion of the UV data (above).

Another interesting observation is that there is no strong difference between the trends seen in the surface potential of surfaces modified by monolayers of molecules from series **1** and **4**; i.e., the phenyl ether group does not have that large an effect (between 0 and 100 mV in CPD_L). The calculations show that it amplifies the effect of the substituents on the free molecule's dipole moment, initially only slightly (0.2 D), but for the CN derivative by 1 D (cf. Table 4).

The 410 mV decrease in band bending, even larger than that observed earlier by Cohen et al.,[6] means that the surface of the n-Si is now less negatively charged. In our case we have, after the etching and cleaning treatments, a SiO_x-covered Si surface that shows relatively strong band bending. The probable reason is that this surface contains a high density of OH and O^- groups that must more than neutralize the Na^+, likely to be present after these treatments. Upon covering this surface with the silanes, the proportion of these OH and O^- groups on the surface is, apparently, reduced. In part this can be because of formation of Si−O−Si bridges instead of Si−OH and SiO^- terminations of the surface. While for OTS it has been shown that no 1:1 silane to surface binding occurs,[36,55] in favor of better OTS chain-to-chain arrangements, with the much shorter chains used here, this may be different. Comparing the C11 with the C6 or C3 BB results we see that BB for the latter is significantly higher than for the C11 ones. Electronegativity estimates, using also group electronegativity values,[56] show that changing an OH-covered surface to one that is Si−O−Si−$(CH_2)_x$−CH_3-covered should, with increasing x, decrease the surface polarity (i.e., less negative charge on the outside).

Table 7 shows the differences between dipole moment values calculated from the experimentally observed surface potential shifts and those obtained from calculations for the free molecules. For all substitutions except CF_3, CN, and NO_2, this difference is around 2 D. Only when the free molecule dipole moment becomes larger than 5 D does this difference increase. One explanation can be that the layer's overall dipole moment depends on the packing of the molecules on the surface. If the angle θ approaches 90°, then for a given free molecule dipole moment, the experimentally observed ΔV will be much smaller than that predicted on the basis of the free molecule's dipole moment (cf. eq 1). Or, stated otherwise, at high tilt from the normal (θ approaches 90°), the dipole moment values deduced from the experimental ΔV values will be smaller than the theoretical ones.

Conclusions

This study has shown that monolayers, made up of a series of molecules with systematically varied structure, can be formed on SiO_x–Si. We do not see a significant change in surface potential if the length or structure (alkyl vs phenyl ether) of the connecting chain between the attached dipolar unit and the silicon surface is varied. This conclusion agrees with what we can derive from the data of Zehner et al.[16] for arenethiols on Au, where sets of molecules with three different lengths also were studied. They see no trends in CPD_d (i.e., the work function of the modified surface) for the OCH_3-, CH_3-, H-, and CF_3-substituted molecules. The same holds true here (in terms of

CPD_L for the OCH_3, CH_3, and H series). It is thus not at all clear how significant are the monotonic decrease that Zehner et al. find for the F-substituted series and the monotonic increase in CPD_L that we find for the Br and NO_2 series.

While monolayer-forming molecules can be varied to yield different derivatives that span quite a range of (free molecule) dipole moments, beyond a dipole moment of about 5 D the monolayer's quality is adversely affected. We explain this by depolarization. While for atomically modified semiconductor surfaces direct charge transfer to and from the surface is thought to be the primary depolarization mechanism, we did not see evidence for this (from the BB data). Rather, here a change in monolayer order, expressed as a change in molecule conformation and, possibly, also a decrease in coverage (but beyond the limited accuracy we have), appears to be the mechanism that decreases the net molecular dipole moment in the monolayer.

The disorder in the monolayer can be understood by realizing that the driving force for it is the dipole−dipole interaction energy between the molecules. The closer the molecules are packed and the higher their dipole moments, the stronger this interaction. It is possible that this effect will be smaller if the molecules are either strongly chemically bound to the surface or form more rigid, highly organized monolayers (stronger van der Waals interaction between the molecules). The latter is unlikely at the level of organization reached here, as we did not observe significant differences between molecules with different phenyl ether chain lengths, but may be important for better ordered films. While in such cases as well we expect a reduction in dipole moment of neighboring molecules, other mechanisms may become dominant. Experiments to explore these and other aspects of molecular chemical surface modifications of semiconductors are underway in our laboratories.

Acknowledgment. We thank the Israel Science Foundation and the Israel Science Ministry for partial financial support. D.C. also thanks the G.M.J. Schmidt Minerva Centre for Supramolecular Chemistry, the Philip M. Klutznick Research Fund, and the Delores & Eugene M. Zemsky John Hopkins−Weizmann Program for partial support. C.N.S. thanks the Deutsche-Israelische Program (DIP) for support.

Supporting Information Available: Purification (distillation or chromatography), yields, and characterization of the remaining olefins and distillation conditions, yields, and characterization of the remaining silanes. This information is available free of charge via the Internet at http://pubs.acs.org.

References and Notes

(1) Evans, S. D.; Urankar, E.; Ulman, A.; Ferris, N. *J. Am. Chem. Soc.* **1991**, *113*, 4121−4131.

(2) Bruening, M.; Moons, E.; Yaron-Marcovich, D.; Cahen, D.; Libman, J.; Shanzer, A. *J. Am. Chem. Soc.* **1994**, *116*, 2972−2977.

(3) Sagiv, J. *J. Am. Chem. Soc.* **1980**, *102*, 92−98.

(4) Ulman, A. *Chem. Rev.* **1996**, *96*, 1533−1554.

(5) Cohen, R.; Ashkenasy, G.; Shanzer, A.; Cahen, D. Grafting Molecular Properties onto Semiconductor Surfaces. In *Semiconductor electrodes & photoelectrochemistry*; Licht, S., Ed.; Wiley-VCH: Weinheim, Germany, 2001; Vol. 6, Chapt. 2.3.

(6) Cohen, R.; Zenou, N.; Cahen, D.; Yitzchaik, S. *Chem. Phys. Lett.* **1997**, *279*, 270−274.

(7) Ashkenasy, G.; Cahen, D.; Cohen, R.; Shanzer, A.; Vilan, A. *Acc. Chem. Res.* **2002**, *35*, 121−128.

(8) Oliveira, O. N.; Taylor, D. M.; Lewis, T. J.; Salvagno, S.; Stirling, C. J. M. *J. Chem. Soc., Faraday Trans. 1* **1989**, *85*, 1009−1018.

(9) Bruening, M.; Cohen, R.; Guillemoles, J. F.; Moav, T.; Libman, J.; Shanzer, A.; Cahen, D. *J. Am. Chem. Soc.* **1997**, *119*, 5720−5728.

(10) The sign of the molecular dipole is chosen arbitrarily to be positive if the positive pole of the dipole points away from the binding group, i.e., from the surface (after binding). Note that in eq 2 we use metric units for the dipole (coulomb·meter); $1\ D = 3.3 \times 10^{-30}$ C·m.

(11) Ulman, A. *Adv. Mater.* **1990**, *2*, 573−582.

(12) Bergveld, P. *Sens. Actuator A: Phys.* **1996**, *56*, 65.

(13) Baptiste, A.; Gibaud, A.; Bardeau, J. F.; Wen, K.; Maoz, R.; Sagiv, J.; Ocko, B. M. *Langmuir* **2002**, *18*, 3916−3922.

(14) Ishii, H.; Sugiyama, K.; Eisuke, I.; Seki, K. *Adv. Mater.* **1999**, *11*, 605−625.

(15) Evans, S. D.; Ulman, A. *Chem. Phys. Lett.* **1990**, *170*, 462−466.

(16) Zehner, R. W.; Parsons, B. F.; Hsung, R. P.; Sita, L. R. *Langmuir* **1999**, *15*, 1121−1127.

(17) Chechik, V.; Crooks, R. M.; Stirling, C. J. M. *Adv. Mater.* **2000**, *12*, 1161−1171.

(18) Flink, S.; van Veggel, F. C. J. M.; Reinhoudt, D. N. *J. Phys. Org. Chem.* **2001**, *14*, 407−415.

(19) Allara, D. L.; Parikh, A. N.; Rondelez, F. *Langmuir* **1995**, *11*, 2357−2360.

(20) Balachander, N.; Sukenik, C. N. *Langmuir* **1990**, *6*, 1621−1627.

(21) Surplice, N. A.; D'Arcy, R. J. *J. Phys. E: Sci. Instrum.* **1970**, *3*, 477−482.

(22) Besocke, K.; Berger, S. *Rev. Sci. Instrum* **1976**, *47*, 840−842.

(23) Kronik, L.; Shapira, Y. *Surf. Sci. Rep.* **1999**, *37*, 1−206.

(24) Bruening, M.; Moons, E.; Cahen, D.; Shanzer, A. *J. Phys. Chem.* **1995**, *99*, 8368−8373.

(25) Gershevitz, O.; Sukenik, C. N.; Ghabboun, J.; Cahen, D. *J. Am. Chem. Soc.* **2003**, *125*, 4730−4731.

(26) Barness, Y.; Gershevitz, O.; Sekar, M.; Sukenik, C. N. *Langmuir* **2000**, *16*, 247−251.

(27) Stewart, J. J. P. *J. Comput. Chem.* **1989**, *10*, 221−264.

(28) Stewart, J. J. P. *J. Comput. Chem.* **1989**, *10*, 209−220.

(29) Becke, A. D. *J. Chem. Phys.* **1993**, *98*, 5648−5652.

(30) Lee, C.; Yang, W.; Parr, R. G. *Phys. Rev. B* **1988**, *37*, 785−789.

(31) Frisch, M. J., Trucks, G. W., Schlegel, H. B., Scuseria, G. E., Robb, M. A., Cheeseman, J. R., Zakrzewski, V. G., Montgomery, J. J. A., et al. *Gaussian 98*, Revision A.7 ed.; Gaussian, Inc: Pittsburgh, PA, 1998.

(32) Young, D. *Computational chemistry, a practical guide for applying techniques to real-world problems*; Wiley: New York, 2001.

(33) Dunning, T. H., Jr. *J. Chem. Phys.* **1989**, *90*, 1007−1023.

(34) De Proft, F.; Martin, J. M. L.; Geerlings, P. *Chem. Phys. Lett.* **1996**, *250*, 393−401.

(35) Fuentealba, P.; Preuss, H.; Stoll, H.; Von Szentpály, L. *Chem. Phys. Lett.* **1989**, *89*, 418−422.

(36) Wang, Y.; Lieberman, M. *Langmuir* **2003**, *19*, 1159−1167 and references therein.

(37) Netzer, L.; Iscovici, R.; Sagiv, J. *Thin Solid Films* **1983**, *99*, 235−241.

(38) Netzer, L.; Iscovici, R.; Sagiv, J. *Thin Solid Films* **1983**, *100*, 67−76.

(39) Wasserman, S. R.; Tao, Y.-T.; Whitesides, G. M. *Langmuir* **1989**, *5*, 1074−1087.

(40) Vallant, T.; Kattner, J.; Brunner, H.; Mayer, U.; Hoffmann, H. *Langmuir* **1999**, *15*, 5339−5346.

(41) Chernyshova, I. V.; Hanumanta Rao, K. *J. Phys. Chem. B* **2001**, *105*, 810−820.

(42) Sze, S. M. *Physics of semiconductor devices*, 2nd ed.; Wiley: New York, 1981.

(43) Bastide, S.; Butruille, R.; Cahen, D.; Dutta, A.; Libman, J.; Shanzer, A.; Sun, L.; Vilan, A. *J. Phys. Chem.* **1997**, *101*, 2678−2684.

(44) Lee, S. H.; Puck, A.; Graupe, M.; Colorado, R., Jr.; Shon, Y.-S.; Lee, T. R.; Perry, S. S. *Langmuir* **2001**, *17*, 7364−7370.

(45) Robin, M. B. *Higher Excited States of Polyatomic Molecules*; Academic: New York, 1975; Vol. 2.

(46) Jaffe, H. H.; Orchin, M. *Theory and Applications of Ultraviolet Spectroscopy*; Wiley: New York, 1966.

(47) Brillson, L. J. *Contacts to semiconductors; Fundamentals and technology*; Noyes: Park Ridge, NJ, 1993.

(48) Spicer, W. E.; Gregory, P. E.; Cgye, P. W.; Babalola, I. A.; Sukegawa, T. *Appl. Phys. Lett.* **1975**, *27*, 617−620.

(49) Mönch, W. *Semiconductor surfaces and interfaces*, 2nd ed.; Springer: Berlin, 1995.

(50) Luth, H. *Surfaces and Interfaces of Solid Materials*, 3rd ed.; Springer: Berlin, 1998.

(51) Duchet, J.; Gerard, J.-F.; Chapel, J.-P.; Chabert, B. *Compos. Interfaces* **2001**, *8*, 177−187.

(52) Fenter, P.; Eberhardt, A.; Liang, K. S.; Eisenberger, P. *J. Chem. Phys.* **1997**, *106*, 1600−1608.

(53) Khanova, L. A.; Evstefeeva, Y. E. *Russ. J. Electrochem. (Elektrokhim.)* **2002**, *38*, 44−48.

(54) Wolf, K. V.; Cole, D. A.; Bernasek, S. L. *Anal. Chem.* **2002**, *74*, 5009−5016.

(55) Maoz, R.; Sagiv, J. *Supramol. Sci.* **1995**, *2*, 9−24.

(56) Huheey, J. E. *Inorganic Chemistry*, 3rd ed.; Harper: New York, 1983.